

Interface barriers at the interfaces of polar GaAs(111) faces with Al₂O₃

H. Y. Chou, E. O'Connor, P. K. Hurley, V. V. Afanas'ev, M. Houssa et al.

Citation: *Appl. Phys. Lett.* **100**, 141602 (2012); doi: 10.1063/1.3698461

View online: <http://dx.doi.org/10.1063/1.3698461>

View Table of Contents: <http://apl.aip.org/resource/1/APPLAB/v100/i14>

Published by the [American Institute of Physics](#).

Related Articles

Observation and simulation of hard x ray photoelectron diffraction to determine polarity of polycrystalline zinc oxide films with rotation domains

J. Appl. Phys. **111**, 033525 (2012)

Valence band dependence on thermal treatment of gold doped glasses and glass ceramics

J. Appl. Phys. **111**, 034701 (2012)

Polarity-dependent photoemission spectra of wurtzite-type zinc oxide

Appl. Phys. Lett. **100**, 051902 (2012)

Growth and valence band offset measurement of PbTe/InSb heterojunctions

Appl. Phys. Lett. **100**, 052108 (2012)

Photoemission microscopy study of the two metal-insulator transitions in Cr-doped V₂O₃

Appl. Phys. Lett. **100**, 014108 (2012)

Additional information on *Appl. Phys. Lett.*

Journal Homepage: <http://apl.aip.org/>

Journal Information: http://apl.aip.org/about/about_the_journal

Top downloads: http://apl.aip.org/features/most_downloaded

Information for Authors: <http://apl.aip.org/authors>

ADVERTISEMENT



HAVE YOU HEARD?

Employers hiring scientists
and engineers trust
physicstoday JOBS



<http://careers.physicstoday.org/post.cfm>

Interface barriers at the interfaces of polar GaAs(111) faces with Al₂O₃

H. Y. Chou,^{1,a)} E. O'Connor,² P. K. Hurley,² V. V. Afanas'ev,¹ M. Houssa,¹ A. Stesmans,¹ P. D. Ye,³ and S. B. Newcomb⁴

¹Department of Physics and Astronomy, University of Leuven, Celestijnenlaan 200D, B-3001 Leuven, Belgium

²Tyndall National Institute, University College Cork, Lee Maltings, Prospect Row, Cork, Ireland

³School of Electrical and Computer Engineering and Brick Nanotechnology Center, Purdue University, West Lafayette, Indiana 47907, USA

⁴Glebe Scientific Ltd., Newport, Tipperary, Ireland

(Received 15 December 2011; accepted 12 March 2012; published online 2 April 2012)

Internal photoemission measurements of barriers for electrons at interfaces between GaAs(111) and atomic-layer deposited Al₂O₃ indicate that changing the GaAs polar crystal face orientation from the Ga-terminated (111)A to the As-terminated (111)B has no effect on the barrier height and remains the same as at the non-polar GaAs(100)/Al₂O₃ interface. Moreover, the presence of native oxide on GaAs(111) or passivation of this surface with sulphur also have no measurable influence on the GaAs(111)/Al₂O₃ barrier. These results suggest that the orientation and composition-sensitive surface dipoles conventionally observed at GaAs surfaces are effectively compensated at GaAs/oxide interfaces. © 2012 American Institute of Physics. [<http://dx.doi.org/10.1063/1.3698461>]

Degraded electron transport properties of A_{III}B_V semiconductor materials at the interfaces with insulators remain a major obstacle hindering development of high-mobility channel structures for future generations of metal-oxide-semiconductor (MOS) devices. Recently, a significantly improved MOS transistor performance was achieved by replacing the traditional (100)GaAs or In_{0.53}Ga_{0.47}As surface orientation by the polar (111)A (Ga or In-rich) crystal face in combination with thermal atomic-layer deposition (ALD) of insulating Al₂O₃.^{1,2} Moreover, the pre-ALD surface treatment in (NH₄)₂S leads to further enhancement of the electron mobility suggesting a lower scattering rate. These results were explained by elimination of hypothetically present interface dipoles, operating as the major factor in electron scattering.² Indeed, GaAs surface dipoles are long known for their strong sensitivity to the composition and processing of the surface.³⁻⁶

However, if applied to an interface, the surface dipole concept must be extended beyond the first layer of interatomic bonds: A charge transfer may also occur between atomic layers located further away from the semiconductor surface plane which might give rise to an additional contribution(s) to the electrostatic potential. Aiming at evaluation of these *interface dipoles*, we addressed the effect of GaAs crystal face orientation, (100) *versus* (111)A (Ga-terminated) and (111)B (As-terminated), as well as of surface chemical treatment on the interface barrier height for electrons between GaAs and ALD-grown Al₂O₃. Within an accuracy of 0.1 eV, we found no measurable contribution of orientation-dependent dipoles, suggesting that the crystal face sensitive charge transfers in the first layer of GaAs-oxide bonds⁷ are compensated by the dipole moments stemming from the next-to-the-first atomic layers at the GaAs/Al₂O₃ interfaces.

In the present work we address the possible impact of both the GaAs crystal face orientation and the surface chemical treatment on the dipole component of the interface barrier with ALD Al₂O₃ insulator films. The samples were

prepared on both n- or p-type GaAs single crystals with dopant concentration of $\approx 6 \times 10^{17} \text{ cm}^{-3}$ and, for each dopant type, two polar surface plane orientations, GaAs(111)A (Ga-terminated) and GaAs(111)B (As-terminated) were explored. This set of samples is contrasted with the previously studied case of the non-polar GaAs(100) face.⁸ Three different GaAs surface conditions were compared: A surface covered with native oxide, a surface with native oxide on passivated by (NH₄)₂S treatment (20 min in a 10% polysulfide water solution at room temperature),^{2,9} and a surface from which native oxides were removed by HCl cleaning (3.7% water solution) followed by the above indicated (NH₄)₂S treatment. Insulating Al₂O₃ films of 20 nm thickness were deposited on these surfaces at 300 °C by ALD using Al(CH₃)₃ and H₂O precursors with a Al(CH₃)₃ pulse being injected first. Cross-sectional transmission electron microscopy (TEM) analysis indicates that the samples obtained by ALD of Al₂O₃ onto native GaAs oxide for both the A and B faces of GaAs(111) [see examples shown in panels (a) and (b) in Fig. 1] exhibit a ~ 1 -nm thick interfacial layer (IL). Though the HCl etching of the native oxide enhances the GaAs surface roughness, TEM images obtained under different defocusing conditions suggest that the IL becomes thinner [panel (c)] or even undetectable [panel (d)] in the sulphur passivated samples, in this way indicating structural differences of the interfaces as affected by the pre-ALD GaAs surface treatment. More TEM images can be found in the supplemental material.¹⁰

The energy barrier height for electrons at the GaAs/Al₂O₃ interfaces was determined using the spectroscopy of internal photoemission (IPE) of electrons from the valence band (VB) of GaAs into the conduction band (CB) of the Al₂O₃ insulator.¹¹ These measurements were performed at room temperature on MOS capacitors fabricated by thermoresistive evaporation of semitransparent (13-15-nm thick) Au electrodes of 0.5 mm² area onto the Al₂O₃ layer. The photocurrent across the oxide was measured as a function of photon energy ($h\nu$) in the spectral range from 2.0 to 6.8 eV and then recalculated to the quantum yield (Y) by normalizing to the incident photon flux. The interface barrier height (Φ) was

^{a)}Electronic mail: HsingYi.Chou@fys.kuleuven.be.

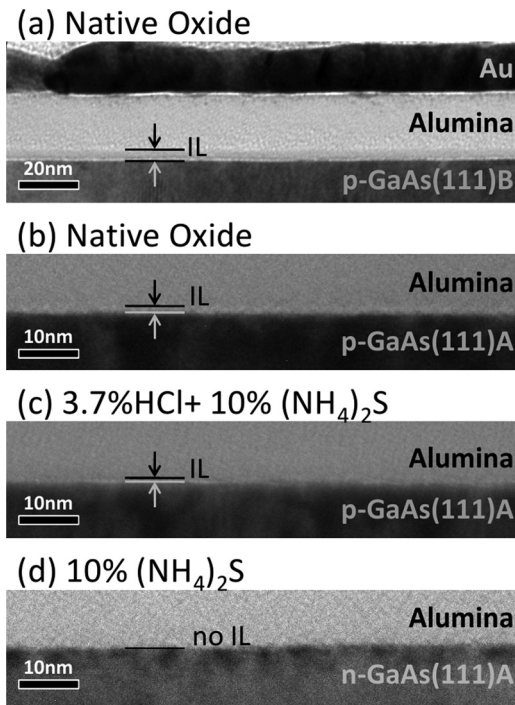


FIG. 1. Cross-sectional TEM images of the interfaces prepared by ALD of Al_2O_3 onto p-type GaAs(111)A and GaAs(111)B surfaces covered with native oxide [panels (a) and (b), respectively] and of the p-GaAs(111)A/ Al_2O_3 interface prepared by etching the native oxide in HCl followed by sulphur passivation (c). For comparison is shown the image of an IL-free interface obtained on a sulphur passivated n-GaAs(111)A surface (d).

inferred from the dependence of Y on $h\nu$ as the spectral threshold of electron IPE.^{12,13}

Semi-logarithmic plots of the IPE yield spectra measured under +2 V bias on the metal in GaAs(111)/ Al_2O_3 /Au samples with different pre-ALD GaAs surface treatment are compared in Fig. 2 for both the (111)A and (111)B GaAs faces. The spectra are seen to be modulated by the features universally observed at $h\nu \approx 4.4$ and $h\nu \approx 4.9$ eV which correspond to the direct optical transitions between high sym-

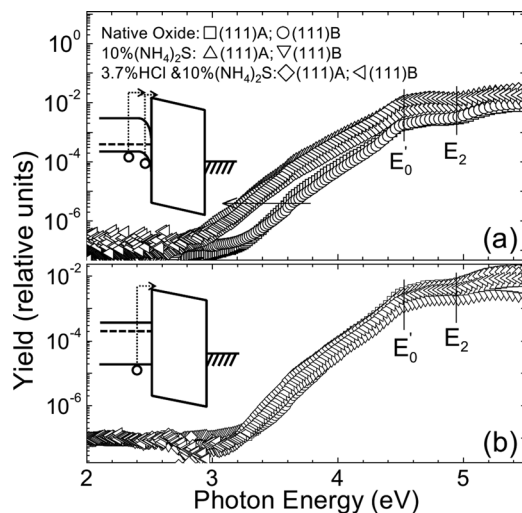


FIG. 2. Semi-logarithmic spectral plots of the IPE yield as a function of photon energy measured, under +2.0 V bias applied to the Au electrode, on p-type (a) and n-type (b) GaAs(111)/ Al_2O_3 /Au samples for different surface orientations and pre-ALD treatments. The vertical lines indicate energies of optical singularities in the GaAs crystal. Insets show a schematic of the observed electron transitions.

metry points in the Brillouin zone of the GaAs crystal at 300 K, [Γ_8^v - Γ_7^c at $E_0' = 4.4$ eV, and X_7 - X_6/Σ_v - Σ_c at $E_2 = 4.9$ eV (Ref. 14)]. These features point to optical excitation in GaAs as the dominant source of photocurrent, thus allowing us to associate this photocurrent with electron IPE from the GaAs VB into the CB of Al_2O_3 . In the case of p-type GaAs [panel (a)], the sulphur passivation is seen to shift the spectral curves towards lower photon energy as indicated by the horizontal arrow. By contrast, in n-type GaAs samples [panel (b)] no such clear shift is observed, suggesting that the $(\text{NH}_4)_2\text{S}$ treatment results in electric field penetration into the p-type MOS samples that leads to a substantial (≈ 0.4 V) variation of the electrostatic potential across the GaAs surface layer over a depth comparable to the mean photoelectron escape depth.¹⁵ This variation in band bending in p-type GaAs corresponds to the shift of the Fermi level from the position close to the VB top in the samples with native oxide towards the CB bottom in the sulphur passivated samples, suggesting that the $(\text{NH}_4)_2\text{S}$ treatment has eliminated the high density of interface traps in the lower portion of the GaAs gap. This results in un-pinning of the Fermi level and allows one to shift it across the GaAs bandgap.¹⁶ Then the positive bias applied to the top metal electrode during IPE measurements would give rise to a large band bending in p-GaAs as illustrated in the inset in Fig. 2(a). Most important, however, is the observation that no measurable change in the IPE spectra occurs when the GaAs(111)A face is changed to GaAs(111)B, irrespective of the initial GaAs surface treatment and the kind of semiconductor conductivity type—even so, as known, with the density of interface defects being significantly different between the samples with native GaAs oxide and those with GaAs surfaces subjected to S-passivation.

The spectral threshold of electron IPE from the GaAs VB into the CB of Al_2O_3 (Φ_e) was determined from $Y^{1/3}$ - $h\nu$ plots^{12,13} by extrapolating the yield to the constant level of the sub-threshold signal, where the latter is related to sample heating by incident light.¹⁷ This is illustrated in Fig. 3 for p-

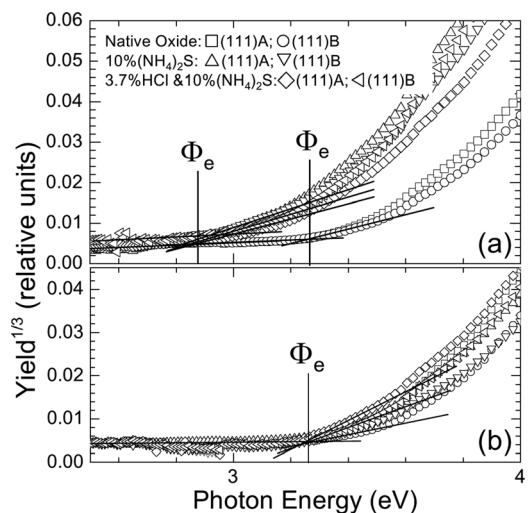


FIG. 3. Cube root of the IPE yield, measured with the average strength of electric field in the oxide of 1 MV/cm, at the interfaces of p-doped (a) and n-doped (b) GaAs(111) samples with an Al_2O_3 layer for different surface orientations and pre-ALD treatments. The vertical lines mark the inferred thresholds, Φ_e , of electron IPE from GaAs into Al_2O_3 .

[panel (a)] and n-type [panel (b)] samples. In p-type samples fabricated by deposition of Al_2O_3 on native oxide (\square , \square), the yield rises up at $\Phi_e \approx 3.25$ eV for both GaAs surface orientations, indicating the absence of crystallographically sensitive dipoles. The same threshold Φ_e is observed on all n-type samples as shown in panel (b). Treatment of p-GaAs in $(\text{NH}_4)_2\text{S}$ results in lowering of the threshold by ~ 0.4 eV which, as already discussed above, is likely to be caused by penetration of electric field into the GaAs photoemitter.

Next, the inferred Φ_e values were plotted as a function of the square root of the electric field (F) across the Al_2O_3 layer (the Schottky plot), calculated by simultaneously taking into account the built-in voltage. The latter was determined as the bias voltage corresponding to zero photocurrent, i.e., to the flat bands in Al_2O_3 . The results are summarized in Fig. 4 which also shows the previously reported results for the non-polar n-GaAs(100) interfaces with an Al_2O_3 layer grown either by thermal (\blacktriangleright) (as applied here) or plasma-assisted (\bullet) ALD.⁸ Except for the S-passivated p-GaAs samples (∇ , \triangle , \diamond , \triangleleft), which, as mentioned, are affected by the electric field penetration in the GaAs, the thresholds of electron IPE at the GaAs(111)A/ Al_2O_3 and GaAs(111)B/ Al_2O_3 interfaces fall (\blacksquare , \square , and the encircled symbols in Fig. 4) on the same trendline as those observed at the GaAs(100)/ Al_2O_3 interfaces (\blacktriangleright , \bullet), indicating that the energy barrier between the top of the GaAs VB and the bottom of the Al_2O_3 CB remains the same. Extrapolation to zero field yields the barrier $\Phi_e(F=0) = 3.4 \pm 0.1$ eV—one coinciding value, irrespective of the GaAs surface orientation and the pre-ALD surface treatment. Moreover, given that defect generation during GaAs oxidation is seen to be a result of strain relief occurring through ejection of surface atoms,¹⁸ oxidation-induced variation of the surface atomic composition may also be excluded as the possible source of interface dipole formation since no Φ_e variation is found at interfaces with different trap density.

From a more general perspective, the results of the present work suggest that the orientation and processing-sensitive surface dipole formation well established before for clean GaAs surfaces^{3–6} cease to work at the interface with an insulating Al_2O_3 layer. The possible explanation of the latter

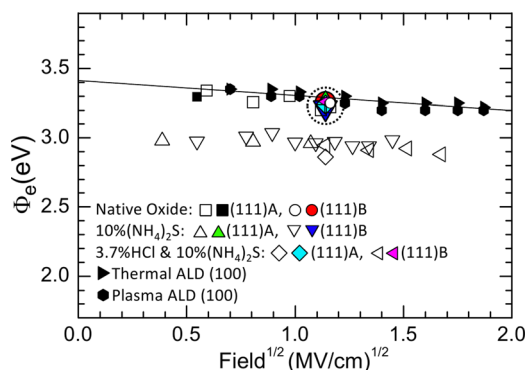


FIG. 4. The Schottky plot of the electron IPE thresholds measured on the differently prepared GaAs(111)/ Al_2O_3 interfaces, on comparison with the values observed at GaAs(100)/ Al_2O_3 interfaces with the oxide grown by thermal (\blacktriangleright) or the plasma-assisted (\bullet) ALD. Filled and open symbols correspond to n-type GaAs and p-type GaAs samples, respectively. Encircled datapoints correspond to the overlapping spectral threshold results as measured on different samples under +2 V bias applied to the top Au electrode. Line illustrates determination of the zero-field barrier.

effect might be related to the fact that, unlike the case of an uncovered GaAs surface, at an interface charge transfer may occur not only between the atoms at the very surface of the semiconductor but also between atomic layers located in the oxide more remote from the geometrical plane of the interface. For instance, in the model proposed in Fig. 11(a) of Ref. 2, the additional partial charges may be positioned on Al atoms making up the layer next to the group VI (oxygen or sulfur) atomic plane. Importantly, this second dipole layer will be of opposite orientation than that formed at the GaAs surface and, hence, will compensate it. As the results of the present work suggest, this compensation appears to be complete within the accuracy of the IPE measurements.

Here, it should be added that this conclusion does not contradict the earlier reported¹⁹ lowering of the interface electron barrier by ≈ 0.3 eV upon high-temperature annealing of $\text{In}_{0.53}\text{Ga}_{0.47}\text{As}(100)/\text{Al}_2\text{O}_3$ entities: This barrier variation is probably caused by the oxide CB bottom shift due to in-diffusion of In or Ga into the Al_2O_3 film since a comparable red shift is also found at the opposite Al/ Al_2O_3 interface in the same MOS structures. Also, the sensitivity of the IPE spectral curves to the GaAs(100) surface treatments²⁰ is unlikely to be due to interface dipoles because, as already discussed in detail,⁸ development of a low energy IPE band correlates with the growth of a narrow gap Ga_2O_3 -like interlayer between GaAs and Al_2O_3 .

From the practical point of view, the revealed absence of significant (>0.1 eV) orientation-sensitive dipoles at GaAs/ Al_2O_3 interfaces represents good news for $\text{A}_{\text{III}}\text{B}_{\text{V}}$ MOS channel design: The MOS devices can be fabricated on the GaAs face delivering the highest carrier mobility without worrying about a dipole-induced threshold voltage shift. Moreover, the non-planar $\text{A}_{\text{III}}\text{B}_{\text{V}}$ MOS transistor design becomes more feasible^{21–23} as no additional compensation is required for potentially different threshold voltage at the differently oriented faces of a 3D channel.

To conclude, the IPE experiments reveal that the electron barrier height between the top of the GaAs VB and the bottom of the Al_2O_3 CB shows no measurable variation when changing the surface orientation of the GaAs substrate crystal and its chemical treatment prior to Al_2O_3 deposition. This result suggests that the surface dipoles known from previous studies at the free GaAs surfaces are largely compensated by charge transfer between atoms in the oxide layer.

The authors acknowledge Ian Povey and Aileen O'Mahony from Tyndall for work on the InGaAs surface preparation and ALD oxide growth and the authors PKH and EO'C gratefully acknowledge the financial support of the Science Foundation Ireland strategic research cluster FORME under Project No. 07/SRC/I1172.

¹M. Xu, Y. Q. Wu, O. Koybasi, T. Shen, and P. D. Ye, *Appl. Phys. Lett.* **94**, 212104 (2009).

²Y. Urabe, N. Miyata, H. Ishii, T. Itatani, T. Maedam T. Yasuda, H. Yamada, N. Fukuhara, M. Hata, M. Yokoyama, N. Taoka, N. Takenaka, and S. Takagi, *Tech. Dig. -Int. Electron Devices Meet.* 6-8 Dec (2010), p. 142.

³I. M. Vitomirov, A. Raisanen, A. C. Finnefrock, R. E. Viturro, L. J. Brillson, P. D. Kirchner, G. D. Prtti, and J. M. Woodall, *Phys. Rev. B* **46**, 13293 (1992); *J. Vac. Sci. Technol. B* **10**, 1898 (1992).

⁴W. Chen, M. Dumas, D. Mao, and A. Kahn, *J. Vac. Sci. Technol. B* **10**, 1886 (1992).

- ⁵R. Duszak, C. J. Palmstrom, and L. T. Florez, Y. N. Yang, and J. H. Weaver, *J. Vac. Sci. Technol. B* **10**, 1891 (1992).
- ⁶I. Jimenez, F. J. Palomares, and J. L. Sacedon, *Phys. Rev. B* **49**, 11117 (1994).
- ⁷G. Hegde, G. Klimeck, and A. Strachan, *Appl. Phys. Lett.* **99**, 093508 (2011).
- ⁸V. V. Afanas'ev, M. Badylevich, A. Stesmans, G. Brammert, A. Delabie, S. Sionke, A. O'Mahony, I. M. Povey, M. E. Pemble, E. O'Connor, P. K. Hurley, and S. B. Newcomb, *Appl. Phys. Lett.* **93**, 212104 (2008).
- ⁹Y. Nanichi, J. Fan, H. Oigawwa, and A. Koma, *Jpn. J. Appl. Phys.* **27**, 2367 (1988).
- ¹⁰See supplementary material at <http://dx.doi.org/10.1063/1.3698461> for additional TEM images.
- ¹¹V. V. Afanas'ev and A. Stesmans, *J. Appl. Phys.* **102**, 081301 (2007).
- ¹²R. J. Powell, *J. Appl. Phys.* **41**, 2424 (1970).
- ¹³J. S. Helman and F. Sanchez-Sinencio, *Phys. Rev. B* **7**, 3702 (1973).
- ¹⁴P. Y. Yu and M. Cardona, *Fundamentals of Semiconductors: Physics and Materials Properties*, 2nd ed (Springer, New York, 1999).
- ¹⁵V. V. Afanas'ev, H. Y. Chou, A. Stesmans, C. Merckling, and X. Sun, *Appl. Phys. Lett.* **98**, 072102 (2011).
- ¹⁶E. O'Connor, B. Rennan, V. Djara, K. Cherkaoui, S. Monaghan, S. B. Newcomb, R. Contreras, M. Milojevic, G. Hughes, M. E. Pemble, R. M. Wallace, and P. K. Hurley, *J. Appl. Phys.* **109**, 024101 (2011).
- ¹⁷R. Williams, *Semiconductors and Semimetals. Volume 6: Injection Phenomena*, edited by R. K. Willardson and A. C. Beer (Academic, New York, 1970), pp. 103–105.
- ¹⁸M. Scarrozza, G. Pourtois, M. Houssa, M. Caymax, A. Stesmans, M. Meuris, and M. M. Heyns, *Appl. Phys. Lett.* **95**, 253504 (2009).
- ¹⁹N. V. Nguyen, M. Xu, O. A. Kirillov, P. D. Ye, C. Wang, K. Cheung, and J. S. Suehle, *Appl. Phys. Lett.* **96**, 052107 (2010).
- ²⁰N. V. Nguyen, O. A. Kirillov, W. Jiang, W. Wang, J. S. Suehle, P. D. Ye, Y. Xuan, N. Goel, K.-W. Choi, W. Tsai, and S. Sayan, *Appl. Phys. Lett.* **93**, 082105 (2008).
- ²¹M. Radosavljevic, G. Dewey, J. M. Fastenau, J. Kavalieros, R. Kotlyar, B. Chu-Kung, W. K. Liu, D. Lubyshev, M. Metz, K. Millard, N. Mukherjee, L. Pan, R. Pillarisetty, W. Rachmady, U. Shah, and Robert Chau, *Tech. Dig.-Int. Electron Devices Meet.* 6-8 Dec (2010), p. 126.
- ²²J. J. Gu, O. Koybasi, Y. Q. Wu, and P. D. Ye, *Appl. Phys. Lett.* **99**, 112113 (2011).
- ²³J. J. Gu, A. T. Neal, and P. D. Ye, *Appl. Phys. Lett.* **99**, 152113 (2011).